

Self-assembled multilayers of gold nanoparticles: nitrate-induced rectification of quantized capacitance charging and effects of alkaline (earth) ions in aqueous solutions

Fengjun Deng and Shaowei Chen*

Department of Chemistry and Biochemistry, University of California, Santa Cruz, California, 95064, USA. E-mail: schen@chemistry.ucsc.edu; Fax: 831-459-2935; Tel: 831-459-5841

Received 8th July 2005, Accepted 21st July 2005

First published as an Advance Article on the web 4th August 2005

Gold nanoparticle multilayers were self-assembled onto an electrode surface by using a dipping method. The particle assemblies exhibited quantized capacitance charging characteristics in aqueous media that were rectified by hydrophobic anions such as PF_6^- , BF_4^- and ClO_4^- , similar to the behavior with the monolayer counterparts. More interestingly, even in the presence of less hydrophobic anions such as NO_3^- , very well-defined single electron transfers were observed voltammetrically with these particle multilayers, a response unseen previously with particle monolayers. This was ascribed, in part, to the enhanced interactions between the particle multilayers and the electrolyte anions as well as the minimization of the structural defects within the particle thin films as compared to the monolayer counterparts. Further studies showed that with particles functionalized with oligo(ethylene oxide) moieties, the particle charge transfer properties were also found to be affected by electrolyte cations, reflected by the variation of the particle molecular capacitance and formal potentials with the nature of the alkaline (earth) metal ions.

Introduction

Monolayer-protected nanoparticles (MPCs) exhibit interesting single-electron transfer characteristics in solutions, the quantized charging to the particle molecular capacitance.^{1–3} The fundamental basis lies in the particle nanosized dimensions which give rise to an attofarad-scale molecular capacitance. Consequently, the energetic barrier for a single electron transfer is significantly greater than the thermal kinetic energy even at ambient temperature.² So far such unique behavior has been observed mostly with gold nanoparticles.¹ Some recent studies have demonstrated that other metal MPCs such as palladium³ and copper⁴ also exhibit similar voltammetric responses, suggesting a universal molecular framework within which nanoparticle-based single electron transistors are attainable.²

In more recent studies,⁵ we discovered that when the particles were immobilized onto electrode surfaces forming organized monolayers, these quantized charging features could be rectified by hydrophobic anions in aqueous media. This unique rectification was reflected in electrochemical measurements where (i) the currents at positive potentials exhibited a series of voltammetric peaks that were ascribed to the quantized capacitance charging of the particle molecules whereas at the negative potential regime, only featureless voltammetric responses were found; and (ii) the currents at positive potentials were significantly greater than those at negative potentials. This behavior of unidirectional current flow was very similar to that of a molecular diode (current rectifier).⁶ This phenomenon was interpreted on the basis of a Randle's equivalent circuit, where the ion-pairing of the positively charged particles (at positive potentials) with hydrophobic electrolyte anions led to the manipulation of the electrode double-layer capacitance and the resulting voltammetric currents. For nanoparticle monolayers, rectified quantized charging has been observed in the presence of PF_6^- , BF_4^- , and ClO_4^- ; whereas in the presence of less hydrophobic ions such as NO_3^- , HSO_4^- , H_2PO_4^- , etc., only featureless responses were observed. It has also been found that the binding of electrolyte anions to the particles

leads to an enhancement of the effective particle molecular capacitance and a cathodic shift of the particle potential of zero charge (PZC).⁵

Using these previous studies⁵ as a point of departure, we carried out further investigations with particle multilayers. It has to be noted that previous electrochemical studies with gold nanoparticle multilayers were mostly limited either to the quantized charging properties in (low-dielectric) organic media,⁷ or focused on the voltammetric characteristics of redox probe molecules embedded within the particle matrices or in the solutions where the particle layers mainly acted as an electron-transfer mediator.⁸ So far no studies have been carried out to investigate the rectified charging properties of gold nanoparticle multilayers in aqueous solutions. By depositing multilayers of nanoparticles onto the electrode surface, it is anticipated that the structural defects within the surface assemblies and the resulting background charging current will be minimized. This will effectively lead to a more hydrophobic surface of the particle assemblies. Since the rectification of particle quantized charging is a consequence of ion pairing between nanoparticles and hydrophobic anions, by increasing the hydrophobicity of the particle assemblies, we may be able to enhance the interactions between the particles and less hydrophobic ions such that quantized charging becomes observable.

The interactions between nanoparticles and electrolyte ions can be further manipulated by chemical functionalizations of the particle molecules. For instance, surface place exchange reactions have been employed to introduce new functional moieties into the particle protecting monolayers and the exact concentration of the new ligands can be readily evaluated by varied spectroscopic techniques.⁹ For instance, it has been found that oligo(ethylene oxide) moieties form helical structures and specifically bind to alkaline (earth) ions, analogous to crown ethers.¹⁰ By incorporating multiple copies of the mercapto-derivatives of ethylene oxide into the particle protecting monolayers *via* exchange reactions, one may then exploit this unique structure for the investigation of the effects of the

interactions between nanoparticles and electrolyte cations on the particle quantized charge transfer chemistry.

In this article, we first report the interesting rectified quantized charging properties of gold nanoparticle multilayers in the presence of relatively "hard" anions such as nitrate, a phenomenon that has not been observed previously with nanoparticle monolayers. Then we extend the studies to nanoparticles functionalized with oligo(ethylene oxide) moieties with a focus on the effects of cationic interactions on the particle quantized charging behavior.

Experimental

Chemicals

Ammonium perchlorate (NH_4ClO_4 , 99.8%, ACROS), lithium nitrate (LiNO_3 , 99%, ACROS), lithium acetate (LiAc , 98%, ACROS), sodium nitrate (NaNO_3 , $\geq 98\%$, ACROS), sodium acetate (NaAc , $\geq 99\%$, ACROS), potassium nitrate (KNO_3 , Fisher), potassium acetate (KAc , 99+%, ACROS), rubidium nitrate (RbNO_3 , 99.8%, ACROS), cesium nitrate (CsNO_3 , 99.9%, ACROS), cesium acetate (CsAc , 99%, ACROS), magnesium nitrate ($\text{Mg}(\text{NO}_3)_2$, $\geq 99\%$, ACROS), magnesium acetate (MgAc_2 , $\geq 99.5\%$, ACROS), strontium nitrate ($\text{Sr}(\text{NO}_3)_2$, $\geq 99\%$, ACROS), barium nitrate ($\text{Ba}(\text{NO}_3)_2$, $\geq 99\%$, ACROS), barium acetate (BaAc_2 , $\geq 99\%$, ACROS), ammonium tetrafluoroborate (NH_4BF_4 , 97%, Aldrich), and potassium perchlorate (KClO_4 , $\geq 99\%$, ACROS) were all used as received. Potassium hexafluorophosphate (KPF_6 , 99%, Aldrich) was re-crystallized twice prior to use. 1-Hexanethiol (C_6SH , 97%, ACROS) and 1-nonanethiol (C_9SH , 96%, ACROS) were also used as received. All solvents were obtained from typical commercial sources and used as received as well. Water was supplied by a Barnstead Nanopure water system ($\geq 18.3 \text{ M}\Omega$).

Two mercapto-derivatives with oligo(ethylene oxide) moieties, $\text{HS}(\text{CH}_2\text{CH}_2\text{O})_2\text{CH}_3$ (EG2SH) and $\text{HS}(\text{CH}_2\text{CH}_2\text{O})_4\text{CH}_3$ (EG4SH), were synthesized and purified by following a literature procedure.¹¹

Nanoparticle synthesis

Gold nanoparticles protected with a monolayer of hexanethiolates or nonanethiolates were synthesized by using a modified Brust protocol.^{9,12} The particles were then subject to fractionation and thermal annealing to reduce the particle core size dispersity. The fractions with an average diameter around 1.6 nm (as determined by transmission electron microscopic measurements) were used in subsequent studies. These particles were denoted as C6Au and C9Au, respectively.

Multiple copies of EG2SH and EG4SH were then introduced into the protecting layers of C6Au and C9Au particles, respectively, by place exchange reactions.⁹ The final concentrations of EG2SH or EG4SH on the particle surfaces were varied by the initial feed ratios and quantitatively evaluated by ^1H NMR measurements. Up to 40% of the original alkanethiolate ligands were replaced by the new ethylene oxide chains, as determined by the ratios of the integrated peak intensities of the protons from the methyl groups *versus* those from the methoxy groups. The resulting particles were denoted as C6AuEG2 and C9AuEG4, respectively.

Nanoparticle multilayer assemblies

Multilayers of the particles synthesized above were then deposited onto a gold electrode surface for electrochemical measurements. Prior to use, a polycrystalline gold disk electrode (sealed in a glass tubing) was first polished with 0.05 μm alumina slurries, followed by sonication in dilute nitric acid, sulfuric acid, and Nanopure water successively. The electrode was then subject to electrochemical etching by rapid potential

sweeps (10 V s^{-1}) in 0.10 M H_2SO_4 within the potential range of +1.2 and -0.2 V for 5 min. The electrode was then rinsed with Nanopure water and ethanol and dried in a gentle stream of nitrogen before a multilayer of particles was deposited onto the electrode surface.

We prepared the particle assemblies by a simple dipping method. First we immersed the electrode into a dichloromethane solution of gold nanoparticles (1 mg mL^{-1}). The electrode was then quickly removed from the solution. As the electrode was wetted with a layer of particle solution, the evaporation of the volatile solvent left a multilayer structure on the electrode surface. A nitrogen stream was used to help remove the moisture that formed during the evaporation process. The number of gold particle layers was estimated by voltammetric measurements, and found to vary typically within a rather narrow range from a few tens to somewhat more than a hundred (*vide infra*).

Electrochemistry

Electrochemical measurements were carried out with a CHI440 electrochemical workstation. A gold electrode with the self-assembled particle multilayers was used as the working electrode (electrode area typically *ca.* 1.0 mm^2), a Ag/AgCl wire and a Pt coil were used as the quasi-reference and counter electrodes, respectively. The potential reference was calibrated by using the formal potential of the redox couple of $\text{K}_3\text{Fe}(\text{CN})_6$ and $\text{K}_4\text{Fe}(\text{CN})_6$, which is $+0.361 \text{ V vs. NHE}$.¹³ All potentials reported herein are converted with reference to NHE. The electrolyte solutions were deaerated for at least 20 min by ultrahigh-purity nitrogen and protected by such a nitrogen atmosphere during the entire experimental procedure.

Results and discussion

Nitrate-induced rectification of particle quantized charging

Fig. 1 shows the cyclic (A, CV) and differential pulse voltammograms (B, DPV) of a C6Au multilayer on a gold electrode surface in varied aqueous electrolyte solutions. One can see that the general features are very similar to those reported previously with gold nanoparticle monolayers,⁵ *i.e.*, at positive potentials (about $0 \sim +1.0 \text{ V vs. NHE}$), a series of well-defined voltammetric peaks emerge, which are attributed to the quantized charging to the double-layer of surface-bound gold particle molecules; whereas at negative potentials, only featureless responses can be found. Such behavior has been termed "ion-induced rectification" of the particle single electron transfers.⁵ Previously, with gold particle monolayers, we observed such rectified quantized charging characteristics only in the presence of hydrophobic anions such as PF_6^- , BF_4^- , and ClO_4^- ions; whereas in the presence of less hydrophobic ions such as NO_3^- , the voltammetric responses were featureless and similar to that of a conventional molecular diode.^{5,6} The discrepancy was interpreted on the basis of a Randle's equivalent circuit where the electrode interfacial capacitance was found to be manipulated by the (ion-pairing) interactions between electrolyte anions and particle molecules. In sharp contrast, with gold particle *multilayers*, the rectified quantized charging behavior can be observed not only in the presence of PF_6^- , BF_4^- , and ClO_4^- but also in solutions containing NO_3^- , as shown in Fig. 1. This seems to suggest that the multilayer structure enhances the interactions between the ions and the particles, since with particle multilayers, it is more likely that the electrode surface will be fully covered and consequently the contribution to background charging will be minimized. By comparing the voltammetric responses, one can see that with particle monolayers,⁵ the overall voltammetric currents increase very rapidly at positive electrode potentials in NO_3^- -containing solutions, suggesting that the electrode double-layer capacitance is very sensitive to electrode polarization and the

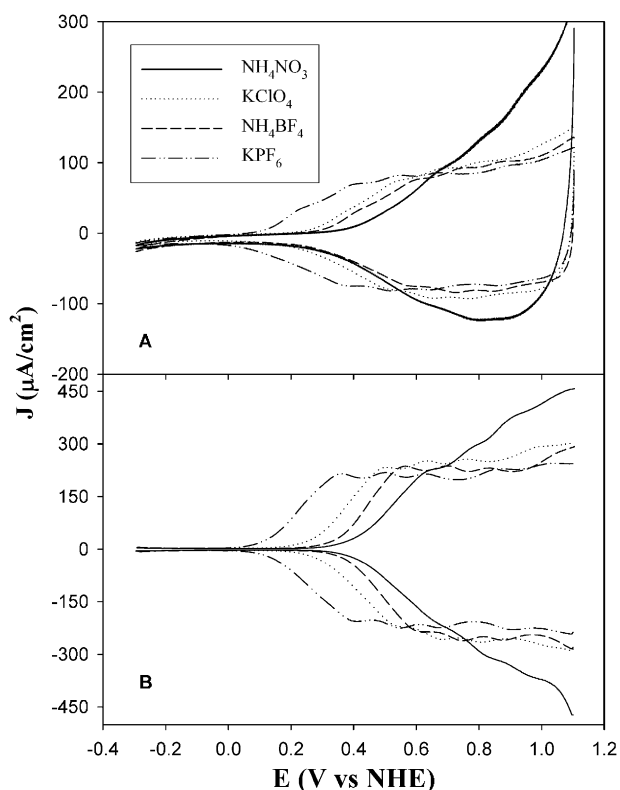


Fig. 1 Cyclic (A, CV) and differential pulse voltammograms (B, DPV) of a C6Au multilayer self-assembled onto a gold electrode surface in varied aqueous electrolytes (0.1 M): NH_4NO_3 , NH_4BF_4 , KClO_4 and KPF_6 . In (A), potential sweep rate 100 mV s^{-1} ; and in (B), DC ramp 4 mV s^{-1} , pulse amplitude 50 mV .

background current becomes the dominating contributions as the electrode potentials become increasingly positive; whereas in the present case with particle multilayers (Fig. 1), the voltammetric currents in the presence of NO_3^- ions show a much shallower rise at positive potentials (though the rise is still somewhat steeper than that with PF_6^- , BF_4^- , or ClO_4^-).

It should be noted that in infrared spectroscopic studies of ion hydration in partially deuterated water (HDO), the maximum of the O–D vibrational band energy was found to decrease in the order of PF_6^- (2664 cm^{-1}), BF_4^- (2647 cm^{-1}), ClO_4^- (2630 cm^{-1}), and NO_3^- (2595 cm^{-1}).¹⁴ All these frequencies are substantially greater than that of bulk water (2509 cm^{-1}), indicating that the water–water interactions are stronger than the water–anion interactions. Thus, one can see that the degree of hydration increases in the order of PF_6^- , BF_4^- , ClO_4^- , and NO_3^- , while the hydrophobicity increases in the reverse order. This observation can also be correlated to the polarization power of the anion (q/r with q being the charge and r the radius of the ion) where a linear relationship has been established.¹⁴ One may therefore suspect that the anion-induced rectification of nanoparticle quantized charging can also be attributed to their hydration and hydrophobicity properties where the interactions between the anions and the hydrophobic particles decrease in the order of PF_6^- , BF_4^- , ClO_4^- , and NO_3^- , as attested in previous⁵ and present voltammetric measurements (more details below).

Since these voltammetric peaks represent a sequence of single electron transfers of the particles to the electrode, the potential spacings (ΔV) between these peaks dictate the corresponding particle capacitance ($C_{\text{MPC}} = e/\Delta V$ with e being the electronic charge).^{1–5} From Fig. 1b, one can see that the average potential separations between neighboring charging peaks are 0.134 V (PF_6^-), 0.132 V (BF_4^-), 0.133 V (ClO_4^-) and 0.142 V (NO_3^-), corresponding to a particle capacitance of 1.19 aF (PF_6^-), 1.21 aF (BF_4^-), 1.20 aF (ClO_4^-), and 1.13 aF

(NO_3^-). Since ion-pairing effectively increases the particle surface dielectric and consequently the particle molecular capacitance, the slightly smaller capacitance in the presence of NO_3^- implies a relatively weak interaction with the particles as compared to the other three anions which are essentially indistinguishable in this regard.

In addition, from Fig. 1 one can see that the voltammetric profiles shift anodically with decreasing hydrophobicity of the anions. This is manifested by the formal potentials of the first quantized charging peaks, $+0.386 \text{ V}$ (PF_6^-), $+0.522 \text{ V}$ (ClO_4^-), $+0.589 \text{ V}$ (BF_4^-), and $+0.647 \text{ V}$ (NO_3^-). This trend is consistent with the above argument that the ion polarization power dictates the ion hydration and interactions of the anions with the nanoparticles (it should be noted that the ionic radii^{5b} are PF_6^- , 0.255 nm ; ClO_4^- , 0.226 nm ; BF_4^- , 0.218 nm ; and NO_3^- , 0.165 nm). This is akin to the effects of specific adsorption of electrolyte anions on electrode potential of zero charge (PZC).¹³ Similar behaviors were also observed in previous results with nanoparticle monolayers.⁵

To estimate the surface coverage (number of layers) of nanoparticles, we varied the potential sweep rates and measured the corresponding voltammetric currents. Fig. 2 (panel A) depicts the cyclic voltammograms of the C6Au multilayers in 0.1 M LiNO_3 at varied scan rates and panel B shows the variation of the first anodic peak currents with potential sweep rate, which exhibits a very good linear relationship. This is in consistency with a surface confined system.¹³ In addition, from the slope, one can estimate the surface coverage of this particle assembly, $1.38 \times 10^{-9} \text{ mol cm}^{-2}$, corresponding to about 42 layers of particles (the coverage for a monolayer of particles is *ca.* $3.30 \times 10^{-11} \text{ mol cm}^{-2}$ by assuming a fully intercalated nanoparticle assembly).

Further examinations were carried out with other electrolyte anions, such as acetate, sulfate, phosphate, halides, *etc.* No quantized charging features were observed in solutions containing any of these anions (not shown).

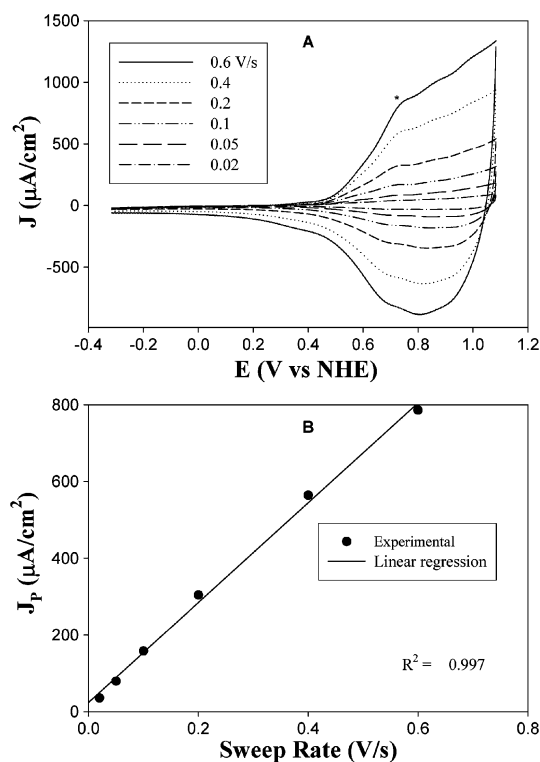


Fig. 2 Cyclic voltammograms (A) of a C6Au multilayer on a gold electrode surface in 0.1 M LiNO_3 solution. The potential sweep rates are shown as figure legends. The variation of the anodic peak currents for the first charging peak (indicated by an asterisk) with potential scan rate is shown in (B).

To quantify the ion-pairing interactions between nitrate ions and surface-immobilized nanoparticles, we varied the concentration of the nitrate ions and measured the corresponding voltammetric responses, as the particle peak potentials were anticipated to shift cathodically with increasing nitrate concentration⁵

$$E_f = E^{o'} + \frac{RT}{n_a F} \ln \frac{K_2}{K_1} - (p - q) \frac{RT}{n_a F} \ln [\text{NO}_3^-] \quad (1)$$

where E_f and $E^{o'}$ are the formal potential in the presence and absence of ion binding, n_a is the (effective) number of electron transfer, K_1 and q (K_2 and p) are the equilibrium constant and the number of anions bound to the reduced (oxidized) forms of the particle molecules, respectively. Fig. 3 shows the (A) CV and (B) DPV of the C6Au multilayer in solutions containing varied concentrations of KNO_3 (with the addition of KAc at an appropriate concentration to maintain the solution ionic strength constant at 0.1 M). One can see that indeed with increasing concentration of the nitrate ions, the overall voltammetric profiles shifted cathodically, as anticipated from eqn (1), akin to previous observations⁵ with particle monolayers in the presence of more hydrophobic anions such as PF_6^- . Fig. 3C depicts the variation of the formal potentials of the particle quantized charging at three different charge states with the natural logarithm of KNO_3 concentration, where symbols are

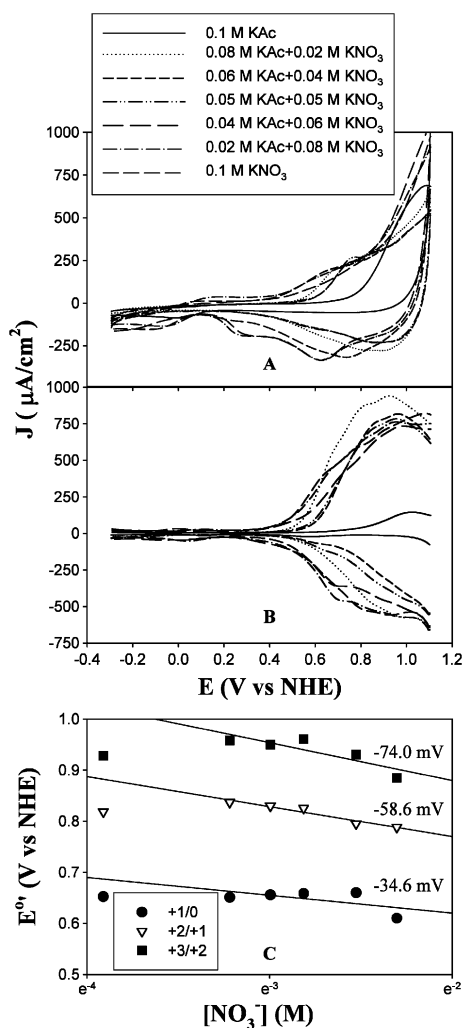


Fig. 3 Cyclic (A, CV) and differential pulse voltammograms (B, DPV) of a C6Au multilayer on a gold electrode surface in aqueous solutions with varied concentrations of KAc and KNO_3 . The total electrolyte concentration is 0.1 M. (C) Variation of the formal potentials of the first three charging peaks with KNO_3 concentration. Symbols are experimental data, and lines are linear regressions. The slopes of the respective linear regression are also shown in the figure.

experimental data, and lines are linear regressions. Reasonably good linearity can be seen for the three charging processes within the concentration range of 0.04 to 0.1 M. The corresponding slopes are -34.6 mV (+1/0) , -58.6 mV (+2/+1) , and -74 mV (+3/+2) , respectively. These values deviate rather significantly from the $-25 \text{ mV } (n_a = 1)$ expected for a 1 : 1 ratio of the number of particle-bound anions and the particle charge states [eqn (1)]. Thus if one assumes that at zero charge state, no ion-pairing occurs, then the numbers of NO_3^- ions bound to the particles at varied charge states are *ca.* 1 ($z = +1$), 3 ($z = +2$), and 6 ($z = +3$). In contrast, for more hydrophobic anions (*e.g.*, PF_6^- , ClO_4^- , and BF_4^-), the ratio is essentially 1 : 1. The observed disparity between NO_3^- and other anions may be, at least in part, accounted for by the different degrees of hydration and hence the effective interactions with the particle molecules, *i.e.*, in these four anions, PF_6^- is least solvated and thus the interactions between the ions and the particles will be most effective; whereas NO_3^- is the most solvated and the interactions with the particles will be discounted by the water solvation layers and hence more ions are needed to accommodate the same electrostatic interactions. This may also explain the substantial deviations when the nitrate concentration is very low (*e.g.*, data points at $[\text{NO}_3^-] = 0.02 \text{ mM}$ in Fig. 3), suggesting a concentration threshold for NO_3^- -induced rectified particle quantized charging.

Effects of alkaline (earth) ions

In the previous⁵ and present studies, the rectification of nanoparticle quantized charging appears to be independent of the cations in aqueous solutions, ranging from “hard” ions such as alkaline (earth) to hydrophobic tetraalkylammonium ions; and the rectified quantized charging features are only observed at positive potentials, suggesting that the interactions between electrolyte anions and particles have dominating impact on the electrode interfacial capacitance and the resulting voltammetric currents. This may again be attributed to the variation of the hydration properties of these ions. As mentioned above, the maxima of the O–D vibration bands blue-shift linearly with increasing polarization power (q/r) of the electrolyte anions; whereas for cations, no continuous dependence on q/r is found.¹⁴ For instance, the O–D vibrational band maxima are found to be around 2533 cm^{-1} for both “hard” alkaline (earth) and “soft” tetraalkylammonium ions, which are only slightly greater than that for bulk water (2509 cm^{-1}), in spite of their wide range of ionic radii. This strongly suggests that, despite their vast disparity in terms of polarization power (hydrophobicity), the presence of these cations does not appear to drastically affect the H-bonding interactions of the surrounding water molecules; and energetically, the hydration structures of these cations do not seem to deviate very much among the series. Such fundamental differences from the anionic properties may account for the lack of cationic rectification of nanoparticle charge transfer in the negative potential regime, because binding with (even hydrophobic) cations results in virtually no change in the interfacial water structure and hence the interfacial double-layer capacitance. In the previous studies,⁵ we proposed that the observed rectification of nanoparticle quantized charging could be interpreted by a Randle’s equivalent circuit where the electrode interfacial double-layer capacitance was varied by the ion-pairing between electrolyte anions and nanoparticle molecules because the adsorption of hydrophobic anions led to the repulsion of water molecules from the electrode surface, as evidenced by electrochemical quartz crystal microbalance (EQ CM) measurements.^{5c} Consequently, the contributions from electrode background charging were minimized and the overall voltammetric currents were dominated by the particle quantized charging. Such ion pairing became more effective at positive potentials with the particles positively charged whereas at

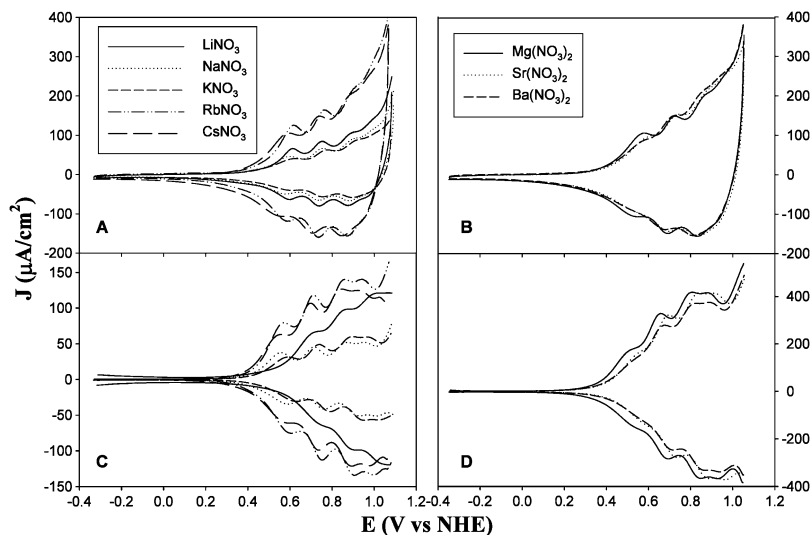


Fig. 4 Cyclic (A, C) and differential pulse voltammograms (B, D) of a C6AuEG2 (13.8%) multilayer in 0.1 M aqueous solutions containing nitrate and different alkali and alkaline earth ions. In (A and B), potential sweep rate 100 mV s^{-1} ; and in (C and D), DC ramp 4 mV s^{-1} , pulse amplitude 50 mV .

negative potentials, ion pairing was not favored. Therefore, a rectified feature was observed.

However, depending on the strength of interactions between the cations and the particles, the nanoparticle molecular capacitance as well as the particle charging potentials might differ as a consequence of the variation of the particle effective dielectric and potential of zero charge (PZC) by ion binding.⁵ One can envision that the interactions between the particles and the cations can be further manipulated by chemical functionalizations of the particle surface. For instance, oligo(ethylene oxide) moieties have been well-known to specifically bind to alkaline (earth) metal ions, akin to crown ethers.¹⁰ Thus by incorporating varied copies of ethylene oxide ligands into the particle protecting monolayers, it is anticipated that the interactions between these particles and alkaline (earth) metal ions can then be readily controlled. Fig. 4 shows some representative CVs (A and B) and DPVs (C and D) of a C6AuEG2 multilayer (exchange ratio 13.8%, 18.5 layers) in a series of nitrate solutions containing different alkaline (A and C) and alkaline earth ions (B and D), where very well-defined rectified quantized charging features can be observed (similar responses were also observed with C9AuEG4 particles at varied exchange ratios, not shown). Rectified voltammetric current profiles were also observed with monolayers of gold nanoparticles protected with a full layer of mercapto-derivatives of ethylene oxide. However, no clear quantized charging features were observed in CV measurements.¹⁵

Fig. 5 (upper panel) depicts the comparison of the particle capacitances, calculated from the potential spacings between neighboring charging peaks that are determined from the DPV measurements, between C6Au and C6AuEG2 particles at varied exchange ratios. One can see that for the C6Au particles, the particle molecular capacitance is virtually invariant among the alkaline and alkaline earth ions except for Sr^{2+} which is *ca.* 8% greater than the rest of the series. Upon the incorporation of the ethylene oxide moieties into the particle protecting monolayers, overall the particle capacitance decreases slightly as compared to that of the original particles. This seems counterintuitive, as the ethylene oxide moieties are more hydrophilic than the alkyl chains and the specific binding to cations should lead to an effective increase of the particle surface dielectric and hence an enhancement of the particle capacitance. The fact that increasing concentration of the EG2 ligands led to a (slight) diminishment of the particle capacitance suggests that the effective dielectric of the particles actually became smaller. This may be partly ascribed to the

more ordered and hence more hydrophobic structure of the particle protecting monolayer as a consequence of specific binding of alkaline (earth) ions to the ethylene oxide moieties.¹⁰ The exact manipulation is dependent upon the EG2 surface concentration. As shown in Fig. 5 (upper panel), at very low (7%) or high (37.8%) exchange, the particle capacitances appear to be smaller than those at 13.8% exchange in all alkaline (earth) ions.

Similar behavior is also observed with C9Au and C9AuEG4 particles (Fig. 5, lower panel). One can see that at 16.3%

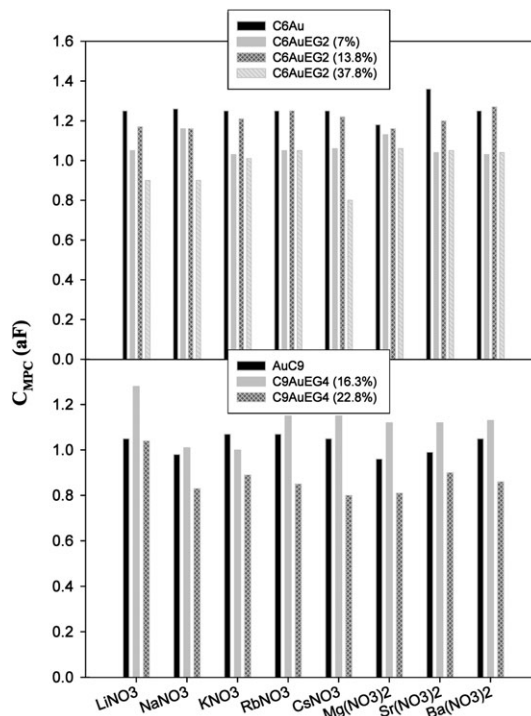


Fig. 5 Molecular capacitance of the gold nanoparticles in nitrate solutions containing different alkaline (earth) ions. The upper panel depicts the data for the C6Au and C6AuEG2 particles at varied exchange ratios while the lower panel for the C9Au and C9AuEG4 counterparts. Data were calculated by using the peak potential positions determined in DPV measurements as exemplified in Fig. 4C and D. The numbers of layers of nanoparticles are C6Au, 42; C6AuEG2 (7%), 27.1; C6AuEG2 (13.8%), 18.5; C6AuEG2 (37.8%), 23.6; C9Au, 10.5; C9AuEG4 (16.3%), 6.2; and C9AuEG4 (22.8%), 18.8.

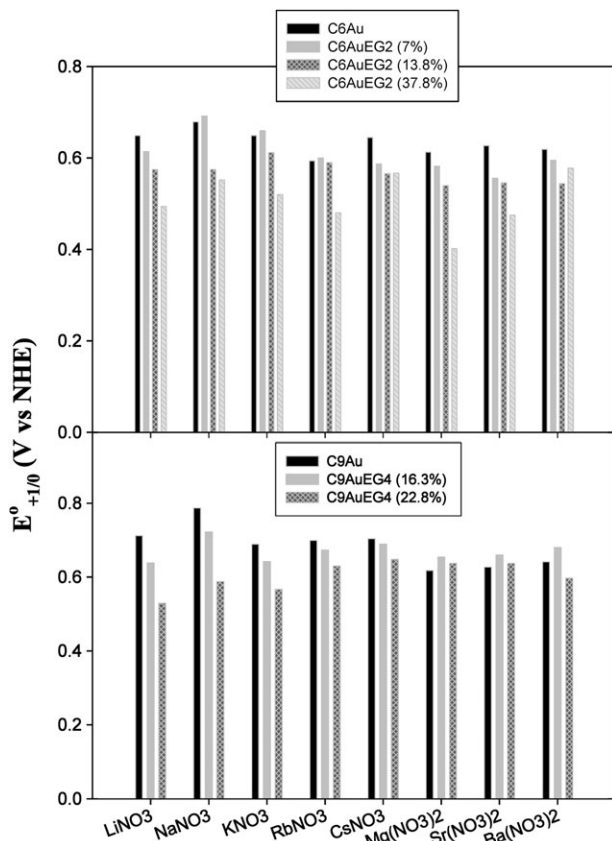


Fig. 6 Formal potentials of the first charging peaks of the gold nanoparticles in nitrate solutions containing different alkaline (earth) ions. The experimental conditions are the same as those identified in Fig. 5.

exchange, the C9AuEG4 particle capacitances are actually somewhat greater than those of C9Au, while at higher exchange (22.8%), the C9AuEG4 particle capacitances are smaller.

From these studies of the binding with electrolyte ions, one can speculate that there are at least two immediate and yet competing impacts of the incorporation of the ethylene oxide moieties into the particle surface layer: On the one hand, an increase of the particle dielectric because of the less hydrophobic nature of the ethylene oxide groups; and on the other, conformational changes of the surface ligands that lead to the exposure of a more hydrophobic surface to the media and hence a decrease of the particle effective dielectric. This is further attested in the measurements of the voltammetric potentials as a function of the EG concentrations, as shown below.

Fig. 6 shows the variation of the formal potentials of the first charging peaks ($E_{+1/0}^{\circ}$) of the C6Au, C6AuEG2, C9Au, and C9AuEG4 nanoparticles in different alkaline (earth) nitrate solutions. The general trend is that with increasing concentration of the ethylene oxide moieties in particle protecting layers, $E_{+1/0}^{\circ}$ shifts cathodically, indicative of an enhanced interaction with the nitrate anions. This is consistent with the above argument that the cation binding to the ethylene oxide moieties leads to an increase of the hydrophobicity of the particle surface layer. Consequently, the binding of the nitrate ions to the particles is enhanced leading to a negative shift of the voltammetric potentials, as observed previously.⁵

It should be noted that the EG2 and EG4 moieties are most likely too short to form stable cyclic complexes with the alkaline (earth) metal ions, and their binding constants with these ions are similar to one another.^{10c} This may explain the lack of a clear trend among the alkaline (earth) ion series for the same particle assemblies, despite some small fluctuations, as observed above in Figs. 5 and 6.

Conclusion

Gold nanoparticle multilayers exhibited rather drastic differences in terms of ion-induced rectification of the particle quantized charging in aqueous solutions, as compared to the monolayer counterparts. With self-assembled multilayers of gold nanoparticles, very well-defined quantized charging characteristics were observed for the first time in NO_3^- -containing solutions. Such discrepancy from the monolayer counterparts was attributable to the minimum structural defects within the particle multilayer assemblies and hence diminishment of background charging currents. In addition, the more hydrophobic multilayer structures might also lead to enhanced interactions between the particles and the electrolyte ions. These observations were correlated to the different degrees of hydration of electrolyte ions as manifested in infrared studies. By incorporating ethylene oxide moieties into the particle protecting monolayers, interactions with electrolyte cations were also examined. The effects were mainly reflected in the variation of the particle molecular capacitance and the formal potentials of the charging peaks as a consequence of the shift of the particle PZC because of the specific interactions between the ethylene oxide moieties and alkaline (earth) metal ions.

Further and more detailed studies are currently underway by using the Langmuir–Blodgett (LB) technique to deliberately control the particle multilayer structures.¹⁶ Results will be reported in due course.

Acknowledgements

The authors thank Dr X. Huang for the donation of some EG2 and EG4 ligands which were used in the initial stage of the research. This work was supported in part by a CAREER Award from the National Science Foundation (CHE-0456130), the Petroleum Research Fund administered by the American Chemical Society (39729-AC5M) and the University of California – Santa Cruz. S.C. is a Cottrell Scholar of Research Corporation.

References

- (a) R. S. Ingram, M. J. Hostetler, R. W. Murray, T. G. Schaaff, J. T. Khoury, R. L. Whetten, T. P. Bigioni, D. K. Guthrie and P. N. First, *J. Am. Chem. Soc.*, 1997, **119**, 9279; (b) S. Chen, R. S. Ingram, M. J. Hostetler, J. J. Pietron, R. W. Murray, T. G. Schaaff, J. T. Khoury, M. M. Alvarez and R. L. Whetten, *Science*, 1998, **280**, 2098; (c) S. Chen, R. W. Murray and S. W. Feldberg, *J. Phys. Chem. B*, 1998, **102**, 9898; (d) J. F. Hicks, A. C. Templeton, S. Chen, K. M. Sheran, R. Jasti, R. W. Murray, J. Debord, T. G. Schaaff and R. L. Whetten, *Anal. Chem.*, 1999, **71**, 3703.
- (a) S. Chen, *J. Electroanal. Chem.*, 2004, **574**, 153; (b) J. Z. Zhang, Z. L. Wang, J. Liu and S. Chen, and G.-Y. Liu, *Self-Assembled Nanostructures*, Kluwer Academic, New York, 2002.
- (a) S. Chen, K. Huang and J. A. Stearns, *Chem. Mater.*, 2000, **12**, 540; (b) Y.-G. Kim, J. C. Garcia-Martinez and R. M. Crooks, *Langmuir*, 2005, **21**, 5485.
- S. Chen and J. M. Sommers, *J. Phys. Chem. B*, 2001, **105**, 8816.
- (a) S. Chen, *J. Am. Chem. Soc.*, 2000, **122**, 7640; (b) S. Chen and R. Pei, *J. Am. Chem. Soc.*, 2001, **123**, 10607; (c) S. Chen and F. Deng, *Proc. SPIE*, 2002, **4807**, 93; (d) S. Chen, R. Pei, T. Zhao and D. J. Dyer, *J. Phys. Chem. B*, 2002, **106**, 1903; (e) S. Chen and F. Deng, *Langmuir*, 2002, **18**, 8942.
- (a) A. Aviram and M. Ratner, *Chem. Phys. Lett.*, 1974, **29**, 277; (b) H. D. Abruña, P. Denisevich, M. Umaña, T. J. Meyer and R. W. Murray, *J. Am. Chem. Soc.*, 1981, **103**, 1; (c) G. P. Kittlesen, H. S. White and M. S. Wrighton, *J. Am. Chem. Soc.*, 1985, **107**, 7373.
- F. P. Zamborini, J. F. Hicks and R. W. Murray, *J. Am. Chem. Soc.*, 2000, **122**, 4515.
- (a) D. I. Gittins, D. Bethell, R. J. Nichols and D. J. Schiffrin, *J. Mater. Chem.*, 2000, **10**, 79; (b) S. Tian, J. Liu, T. Zhu and W. Knoll, *Chem. Mater.*, 2004, **16**, 4103; (c) L. Qian, Q. Gao, Y. Song, Z. Li and X. Yang, *Sensors Actuators B*, 2005, **107**, 303; (d) M. Yamada and H. Nishihara, *C. R. Chim.*, 2003, **6**, 919; (e) P. T. Hammond, *Adv. Mater.*, 2004, **16**, 1271.
- (a) A. C. Templeton, W. P. Wuelfing and R. W. Murray, *Acc. Chem. Res.*, 2000, **33**, 27; (b) R. L. Whetten, M. N. Shafgullin, J.

-
- T. Khoury, T. G. Schaaff, I. Vezmar, M. M. Alvarez and A. Wilkinson, *Acc. Chem. Res.*, 1999, **32**, 397; (c) M. Brust, D. Bethell, D. J. Schiffrin and C. J. Kiely, *Adv. Mater.*, 1995, **7**, 795.
- 10 (a) R. M. Izatt, J. S. Bradshaw, S. A. Nielsen, J. D. Lamb, J. J. Christensen and D. Sen, *Chem. Rev.*, 1985, **85**, 271; (b) J. M. Parker, P. V. Wright and C. C. Lee, *Polym. Commun.*, 1981, **22**, 1305; (c) Y. Sakai, K. Ono, T. Hidaka, M. Tagaki and R. W. Cattrall, *Bull. Chem. Soc. Jpn.*, 2000, **73**, 1165.
- 11 M. Zheng, Z. Li and X. Huang, *Langmuir*, 2004, **20**, 4226.
- 12 M. Brust, M. Walker, D. Bethell, D. J. Schiffrin and R. Whyman, *J. Chem. Soc., Chem. Commun.*, 1994, 801–802.
- 13 A. J. Bard and L. R. Faulkner, *Electrochemical Methods: Fundamentals and Applications*, Wiley, New York, 2nd edn, 2002.
- 14 (a) J. Stangret and T. Gampe, *J. Phys. Chem. A*, 2002, **106**, 5393; (b) M. Śmiechowski, E. Gojło and J. Stangret, *J. Phys. Chem. B*, 2004, **108**, 15938.
- 15 S. D. Jhaveri, D. A. Lowy, E. E. Foos, A. W. Snow, M. G. Ancona and L. M. Tender, *Chem. Commun.*, 2002, 1544.
- 16 F. Deng and S. Chen, unpublished results.